Evaluation of Peroxide Initiators for Radical Polymerization-Based Self-Healing Applications

GERALD O. WILSON,[1,2] JAMES W. HENDERSON,[3] MARY M. CARUSO,[2,4] BENJAMIN J. BLAISZIK,[2,5] PATRICK J. McINTIRE,[4] NANCY R. SOTTOS,[1,2] SCOTT R. WHITE,[2,6] JEFFREY S. MOORE[2,4]

[1]Department of Materials Science and Engineering, University of Illinois at Urbana-Champaign, Urbana, Illinois

[2]Beckman Institute, University of Illinois at Urbana-Champaign, Urbana, Illinois

[3]Department of Molecular and Cellular Biology, University of Illinois at Urbana-Champaign, Urbana, Illinois

[4]Department of Chemistry, University of Illinois at Urbana-Champaign, Urbana, Illinois

[5]Department of Mechanical Science and Engineering, University of Illinois at Urbana-Champaign, Urbana, Illinois

[6]Department of Aerospace Engineering, University of Illinois at Urbana-Champaign, Urbana, Illinois

ABSTRACT: The suitability of various peroxide initiators for a radical polymerization-based self-healing system is evaluated. The initiators are compared using previously established criteria in the design of ring opening metathesis polymerization-based self-healing systems. Benzoyl peroxide (BPO) emerges as the best performing initiator across the range of evaluation criteria. Epoxy vinyl ester resin samples prepared with microcapsules containing BPO exhibited upwards of 80% healing efficiency in preliminary tests in which a mixture of acrylic monomers and tertiary amine activator was injected into the crack plane of the sample after the initial fracture. © 2010 Wiley Periodicals, Inc. J Polym Sci Part A: Polym Chem 48: 2698–2708, 2010

KEYWORDS: bone cement; core-shell polymers; initiators; microencapsulation; radical polymerization; self-healing

INTRODUCTION Self-healing polymers are a newly developed class of smart materials that have the capability to repair themselves when they are damaged without the need for any external intervention. The first example of a self-healing polymer was reported by White et al.[1] This self-healing system was based on microcapsules containing dicyclopentadiene (DCPD) and Grubbs' catalyst particles embedded together in an epoxy matrix. Damage in the form of a crack propagated through the brittle epoxy matrix rupturing the microcapsules to release the DCPD into the crack plane where it came in contact with the Grubbs' catalyst, and initiated a ring opening metathesis polymerization (ROMP), which sealed the crack and restored structural continuity. As this pioneering work was reported, the field of self-healing materials has continued to grow to include new self-healing chemistries such as the PDMS-based[2–4] and solvent-induced chemistries,[5,6] new self-healing concepts using microvascular[7–11] and hollow fiber delivery methods,[12,13] and related nonautonomic technologies such as re-mendable polymers.[14–16]

Self-healing functionality is likely to make the biggest impact in applications such as brittle thermosets and composites where deep damage formed within the structure cannot be easily detected or repaired.[17] If the damage is not repaired at an early stage, it could propagate, eventually leading to catastrophic failures, higher maintenance costs, and lost productivity. Repair solutions designed for these applications must, therefore, be autonomic, arresting the damage at an early stage to prevent further propagation.

For similar reasons to those given for industrial structural applications, biomedical applications are also a suitable target for self-healing functionality. Failure or malfunction in these applications often requires revision surgery. For example, according to the American Academy of Orthopedic Surgeons, the number of primary total hip and total knee replacements reached 234,000 and 478,000, respectively, in 2004, costing patients in the U.S. alone in excess of $20 billion in hospitalization fees. Revision surgeries performed in instances when these implants failed cost U.S. patients in excess of $3 billion in hospitalization fees.[18]

One of the main reasons for failure of cemented arthroplasties is a condition known as aseptic loosening, in which debris particles formed as a result of cement fatigue failure induce inflammatory tissue responses that lead to bone destruction and loosening of the prosthesis.[19,20] The successful demonstration of the microencapsulation-based

self-healing concept in epoxy and epoxy-based structural composites[1,17] in epoxy vinyl ester,[2,21] and in elastomeric materials[4] presents a compelling opportunity to use this concept to solve one of the most costly problems facing orthopedic surgery patients worldwide. Other applications of bone cements that could see significant improvement with the introduction of self-healing technology include: in neurosurgery to repair skull defects; in spinal surgery for injection into the cancellous bone of vertebral bodies in percutaneous vertebroplasty; and in dentistry as part of dental composites, direct filling resins, and fissure sealants.[22–24]

Since its development by Charnley in 1960,[25] the two-part self-polymerizing poly(methyl methacrylate) (PMMA) bone cement (now simply known as bone cement), has emerged as one of the premier synthetic biomaterials in contemporary orthopedics. It is currently the only material used for anchoring prostheses to the contiguous bone in cemented arthroplasties. The cement formulation typically consists of a liquid component, which includes methyl methacrylate (MMA) monomer and a tertiary aromatic amine activator (typically dimethylamino-p-toluidine, DMPT); and a solid component, which includes a polymerization initiator (benzoyl peroxide, BPO), a combination of poly(methyl methacrylate) and poly(styrene-co-methyl methacrylate) beads, and a radiopacifier (e.g., barium sulfate). The liquid and solid components are mixed together just before use to form a grouting which quickly sets as the polymerization of the MMA monomer is initiated.

It is well recognized, however, that bone cement is beset with a number of drawbacks ranging from toxicity of the reactants, which leads to chemical necrosis; the high polymerization exotherm, which leads to thermal necrosis; weak-link zones in the cement construct (bone-cement interface and cement-prosthesis interface); and aseptic loosening.[19,20] These drawbacks often result in complications during and/or after surgery and often lead to revision surgery.

Bone cement research has most recently focused on optimizing cement mixing methods so as to decrease polymerization exotherms, porosity, and viscosity. Decreasing porosity is expected to increase cement resistance to crack propagation and other relevant mechanical properties, whereas decreasing viscosity improves ease of processing as well as the ability of the cement to penetrate into the cancellous bone, thereby increasing the shear strength of the bone-cement interface.[19] Research has also focused on the development of more reactive and less toxic polymerization initiation activators,[26–31] alternative cement monomers,[32–35] and the use of osteoconductive additives for improved cement biocompatibility and mechanical properties of the weak-link zones by supporting the growth of bone cells on the cement construct.[36–38] The recent development of self-healing polymers presents an opportunity for research on extending the lifetime of bone cements. The development of a biocompatible self-healing technology could also lead to applications in biomaterials such as bone cements and dental resins. New chemistries designed for these applications could also be used in other
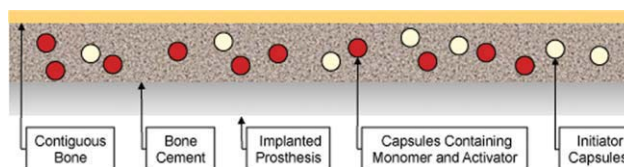
FIGURE 1 Proposed concept for a self-healing bone cement showing the compartmentalization of reactants in microcapsules that would be mixed into the bone cement formulation before application between the prosthesis and the contiguous bone. [Color figure can be viewed in the online issue, which is available at www.interscience.wiley.com.]

nonbiomedical applications such as self-healing reinforced vinyl ester composites, coatings, and adhesives.

Free-radical-initiated polymerization of acrylates stands out as the most attractive chemistry for designing a self-healing system for bone cements since it is identical to the curing chemistries of bone cements and dental resins. A proposed concept for the compartmentalization of this chemistry in a self-healing system is shown in Figure 1. In this dual-capsule concept, damage propagating through the cement in the form of a crack ruptures the microcapsules containing the free-radical initiator as well as those containing the mixture of monomer and activator. The contents of the capsules are then released into the crack plane, where they would react, initiating a free-radical polymerization that would repair the damage and restore structural continuity to the cement.

In this article, we report on the evaluation of various commonly used peroxide initiators aimed at selecting the peroxide initiator best-suited to the diverse demands of a successful self-healing system. On the basis of the characteristics of healing agents successfully used in ROMP-based systems,[39] the evaluation criteria include: thermal stability, reactivity, stoichiometric dependence, and compartmentalization. Chemical stability with the bone cement matrix is evaluated indirectly in preliminary healing performance experiments.

EXPERIMENTAL

Materials
Benzoyl peroxide (**1**, Sigma Aldrich) and lauroyl peroxide (**2**, Sigma Aldrich) were ground into a fine powder before use. Methyl ethyl ketone peroxide (**3**) and 4,N,N-trimethylaniline (**7**) were obtained from Fluka. tert-butyl peroxide (**4**), phenyl acetate, hexyl acetate, and N,N-dimethylaniline (**6**) were obtained from Sigma-Aldrich. tert-butyl peroxybenzoate (**5**) and 4,4′-methylene bis(N,N-dimethyl aniline) (**8**) were obtained from Acros Chemicals. All the above were used as-received from the suppliers. The resin Derakane 510A-40 Epoxy Vinyl Ester (EVE) was generously donated by Ashland Chemicals and used as received.

Thermal Stability of Initiators
Thermal stability of each initiator was evaluated by dynamic differential scanning calorimetry (DSC) experiments (25–300 °C, 10 °C/min) performed on a Mettler-Toledo DSC821[e]. Dynamic experiments were performed under nitrogen

atmosphere, and all DSC experiments were performed in 40 μL aluminum crucibles. Average sample sizes were 5.7 $\pm$ 2.7 mg.

Initiator Reactivity Experiments

The reaction kinetics of the polymerization of the epoxy vinyl ester resin, used in this work as a screening monomer, with each initiator was obtained by dynamic DSC evaluations of 11.8 $\pm$ 3.6 mg samples of epoxy vinyl ester containing initiator (4.13 $\times$ 10^{-4} mol/g). In separate experiments, each initiator was stirred into the resin sample for 5 min at 1000 RPM using a mechanical stirrer before loading the sample into the DSC. To evaluate the reactivity of these initiators with various activators, each activator was added to separate resin samples already containing initiators at varying concentrations. Dynamic DSC evaluations were performed on 21.9 $\pm$ 7.4 mg sample sizes using two concentration combinations of initiator and activator (4.13 $\times$ 10^{-4} mol/g of initiator with 8.25 $\times$ 10^{-5} mol/g of activator; and 8.25 $\times$ 10^{-4} mol/g of initiator with 4.13 $\times$ 10^{-4} mol/g of activator). Samples with liquid activators were prepared by mixing the initiator and resin for 5 min at 1000 RPM, then adding the activator via pipette, stirring for 15 s at 1000 RPM, and loading the sample into the DSC within 118 $\pm$ 20 s after addition of activator. For experiments with the solid activator (4,4-methylene bis(N,N-dimethyl aniline)) that could not be added by pipette, initiator and activator were stirred into EVE separately and the two parts were mixed for 15 s just before loading the sample into the DSC. Samples were loaded within 103 $\pm$ 9 s after combining and stirring the separate initiator and activator solutions together.

Isothermal Experiments

Isothermal DSC experiments were performed at 25 °C, 38 °C, and 50 °C, respectively, for 120 min on samples containing a mixture of EVE and either **1** or **2** at the same two initiator and activator concentrations used in the dynamic experiments. In separate experiments, each initiator was stirred into the resin for 5 min at 1000 RPM, and 19.8 $\pm$ 5.7 mg samples were loaded into the instrument within 119 $\pm$ 21 s after mixing. Resin samples with varying concentrations of initiator (ranging from 4.13 $\times$ 10^{-5} mol/g to 2.06 $\times$ 10^{-4} mol/g) and activator (ranging from 4.13 $\times$ 10^{-6} mol/g to 1.65 $\times$ 10^{-3} mol/g) were evaluated by isothermal DSC at 38 °C (body temperature) for 120 min. Samples weighing 25.4 $\pm$ 9.9 mg were prepared as above and loaded into the DSC within 98 $\pm$ 21 s after addition of the activator. The degree of monomer conversion (α_t) was determined as a function of time using the following equation:

$$\alpha_t = 100 \frac{Q_t}{Q_T} \tag{1}$$

where Q_t is the reaction heat at time t, and Q_T is the total heat of polymerization.[21]

Dynamic Mechanical Analysis

Modulus and T_g were determined from measurements collected on a dynamic mechanical analyzer (DMA, TA RSA 3).

The EVE samples cured with varying ratios of activator (N,N-dimethylaniline) to initiator (BPO or LPO) were cast in 75 mm $\times$ 25 mm $\times$ 2.5 mm silicone molds and cured at RT for 24 h. The samples were cut with a band saw into 30 mm long $\times$ 3.5 mm wide $\times$ 4 mm thick rods. Sample rods were loaded onto a 25 mm three-point bend fixture in the DMA and a dynamic ramp test was performed (25–220 °C at 5 °C/min) under 0.5% strain at a frequency of 1 Hz. Storage modulus (E') at 30 °C, loss modulus (E''), and tan δ were recorded for each sample.

Microencapsulation of Solutions Containing Initiators

The maximum solubility/saturation limit of BPO and LPO initiators at RT (21–23 °C) was determined in phenylacetate and hexyl acetate, respectively, as follows: a constant amount of solvent in a stirring jar was used while the amount of initiator added was increased until no more solid would dissolve. The resulting solubility values are expressed as percentages by weight of solid initiator that dissolved in the respective solvents. Urea-formaldehyde microcapsules[40] were prepared at 500 RPM with a slight modification to the original procedure. The amount of wall-forming materials was cut in half, while the 60 mL of core material remained constant.[41] Capsules with average diameters of 106 $\pm$ 24 μm and 125 $\pm$ 32 μm were produced containing BPO in PA (9.9 wt %) and LPO in hexyl acetate (4.3 wt %), respectively. Bone cement tapered double cantilever beam (TDCB) fracture specimens[42] that contained 10 vol % of microcapsules were prepared and the fracture surfaces were imaged by SEM after sputter-coating with a gold-palladium source.

Sample Preparation and Testing

PMMA simulated bone cement samples were prepared from two parts and were based on the composition of Surgical Simplex® P. The solid part was comprised of a total of 40 g of powder of which 1.7 wt % was BPO (0.68 g) and 10 wt % of initiator capsules (9 wt % BPO in PA). The remainder was PMMA (M_W = 350,000 g/mol, Polysciences). The liquid part (20 mL) was comprised of DMA (2.6 vol %, 520 μL) and the remainder was MMA. The two parts were mixed together and the mixture was quickly transferred to the Teflon® long-groove TDCB mold. The samples were allowed to cure at RT for 24 h after which they were removed from the molds and pin-loaded at 5 μm/s under displacement control to failure, and the fracture surfaces were analyzed by SEM. Epoxy vinyl ester (EVE) long-groove TDCB samples were prepared by stirring 1 wt % BPO into the Derakane 510A-40 resin at 1500 RPM for 5 min, followed by the addition of 0.1 wt % DMA. The mixture was then poured into silicon molds and allowed to cure at RT for 24 h. The central insert section of the sample was prepared with the same matrix materials and procedure as above (EVE, BPO, and DMA) and the appropriate amount of initiator microcapsules (0–10 wt %) were mixed in the resin and poured into molds. The samples were allowed to cure at RT for an additional 24 h after which they were pin-loaded at 5 μm/s under displacement control, and loaded to failure. After removing the specimens from the load frame, a solution containing EVE (1.14 g), MMA (1.07 mL), and 2.1 μL
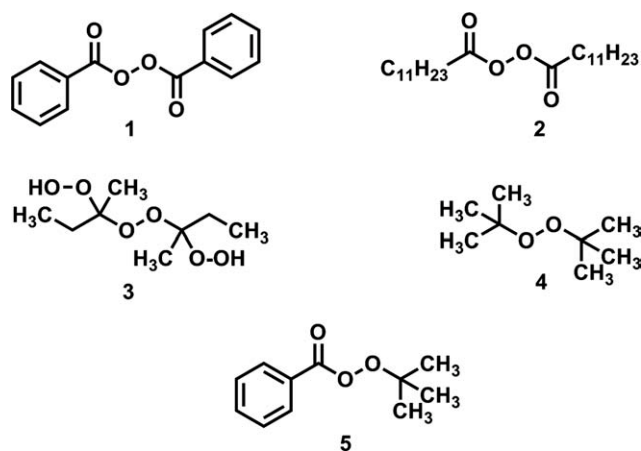
CHART 1 Free radical initiators evaluated.

DMA (0.025 mL) was injected into the crack plane via syringe (25 μL for each TDCB sample). The samples were allowed to heal at RT for 24 h before retesting to failure. Five samples were tested for each data entry.

RESULTS AND DISCUSSION

Selection of Initiators
The peroxide initiators were selected based on a need for a broad range of reactivities, physical properties, and phases represented in the study as well as basic practical screening criteria informed by the intended application. These criteria included toxicity (LD_{50} values $\geq$ 484 mg/kg; a preliminary consideration of potential biocompatibility), water solubility ($\leq$0.5 g/100 mL; low water solubility is essential for facile microencapsulation), melting and boiling points. The initiators selected and their properties are shown in Chart 1 and Table 1,[43] respectively. Initiators **1** and **2** are the most well studied and **1** is already used in existing bone cement formulations, whereas **4** and **5** were most attractive because they were liquids and did not need to be dissolved in a solvent (and hence diluted) before encapsulation. The low melting point of **2** was not considered a concern since it would be dissolved in an appropriate solvent prior to encapsulation.

Thermal Stability
The initiator must survive processing conditions such as microencapsulation, high reaction exotherms due to the curing cement, and an elevated ambient temperature *in vivo*. Relevant thermal transitions such as melting, boiling, and decomposition were compared by dynamic DSC (Fig. 2). The melting and boiling point transitions observed by DSC are consistent with those listed in Table 1, which were used as part of the selection criteria. The onset of decomposition is a more meaningful parameter for assessing thermal stability in a self-healing system. The onset temperature of a thermal event is defined as the intersection between the tangent to the maximum rising slope of a DSC curve and the extrapolated sample baseline.[44] In the case of **1**, the melting point transition is adjacent to the decomposition transition (onset

= 109 °C). Initiator **2** exhibited the earliest onset of decomposition (onset T = 86 °C), suggesting more facile thermal cleavage of O—O peroxide bonds. With temperatures in a curing cement mantle typically in the range of 67–124 °C depending on the formulation,[19] some decomposition of **1**, **2**, and **5** would be likely if incorporated into the cement as part of a self-healing system. However, we expect that a sufficient amount of initiator will survive the cement curing process to initiate healing agent polymerization during a healing event. Initiator **4** was the only initiator that did not decompose during the temperature range of the evaluation (25–300 °C) suggesting that this initiator may not initiate a polymerization during a healing event, even in the presence of an activator.

Comparison of Polymerization Kinetics by DSC
Polymerization of healing agent released into a propagating crack plane must occur rapidly before the healing agent is lost by evaporation, diffusion, or absorption into the matrix. The polymerization also cannot be so fast that it impedes the flow of the healing agent across the entire crack face. The ability of the initiators to initiate polymerization of acrylic monomers was evaluated using Derakane® 510A-40 epoxy vinyl ester (EVE) resin as the screening monomer. The EVE resin was chosen as the screening monomer due to the presence of methacrylate groups which are also present in MMA, the monomer used in standard bone cement formulations, and its similarity to bisphenol-A diglycidyl dimethacrylate (Bis-GMA), which is used in various restorative dental materials.[45]

In the absence of activators, the average onset temperatures for polymerization of the EVE resin closely mirrored the average onset temperatures for decomposition, with **2** and **4** exhibiting the lowest and highest onset temperatures of polymerization, respectively (Fig. 3). The reactivities of the initiators with three different activators (Chart 2) were also evaluated. In general, the addition of activators either lowered, or had no effect on the onset temperature of polymerization (Table 2). The onset temperature of polymerization with **1** was most affected by the addition of activator. As the concentration of initiator and activator increased, the onset temperature of polymerization decreased. Initiator **2** did not demonstrate a high level of reactivity with **6** at the lower concentration, as indicated by a minimal change in onset temperature relative to thermal polymerization of the epoxy

TABLE 1 Relevant Properties of Evaluated Initiators

| Initiator	Heat of Decomposition (kJ/mol)	Total Heat 25–300 °C (kJ/mol)	Average Onset T (°C)
1	N/A	295.1 (6.6)	109.1 (0.1)
2	277.5 (15.4)	192.2 (9.4)	85.8 (0.3)
3	107.7 (8.3)	107.7 (8.3)	128.1 (4.8)
4	N/A	−49.4 (3.3)	109.2 (1.0)
5	214.8 (0.2)	214.8 (0.2)	112.0 (13.7)
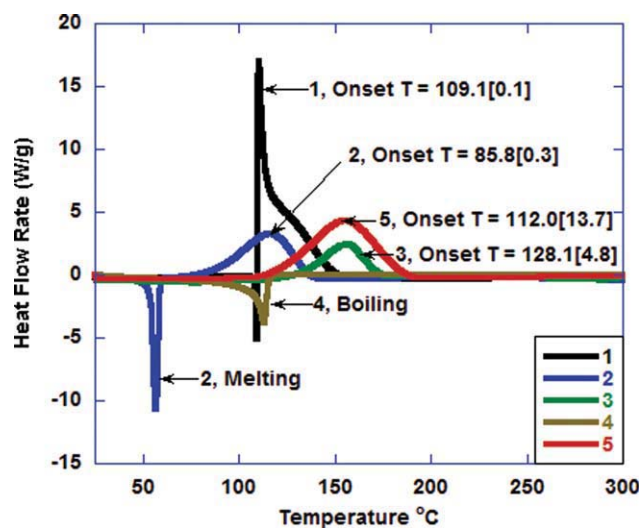
FIGURE 2 DSC evaluation of the thermal stability of initiators. The average onset temperature (with one standard deviation based on three trials included in brackets) of decomposition has been included for all initiators where appropriate.

vinyl ester resin (Fig. 3). However, when the concentration of **2** was increased two-fold and that of **6** increased five-fold, the onset temperature significantly decreased to 70 °C. In addition, **1** and **2** appeared to react faster with **7** and **8** than with **6**. This observation is consistent with increased nucleophilicity of the tertiary amine due to donation of electron density from the methyl functionality in the *para* position of the benzene ring of **7** by hyperconjugation. Similarly, **8** demonstrated a higher level of reactivity with these initiators as a result of its increased nucleophilicity and bifunctionality. The average onset temperature for polymerization with **3** decreased with the addition of activator, but decreased only
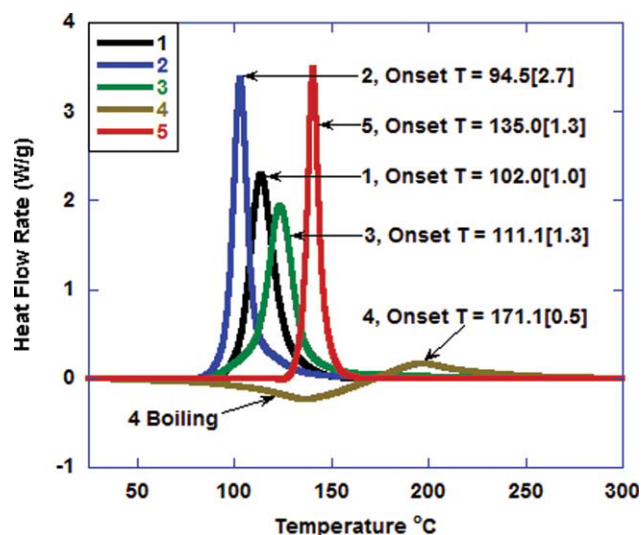
FIGURE 3 DSC evaluation of the reactivity of initiators with EVE. The average onset temperature of polymerization (with one standard deviation based on three trials included in brackets) of the resin by each initiator is included.
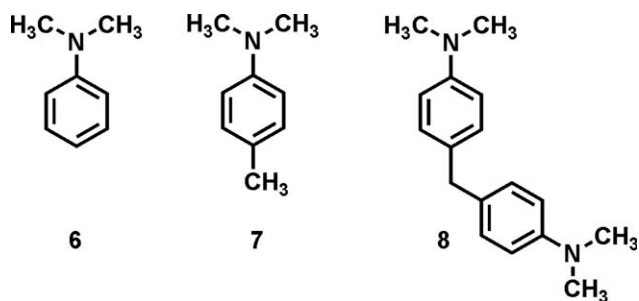
CHART 2 Corresponding activators evaluated.

marginally with increased concentration of both initiator and activator in comparison to the decreases observed for **1** and **2**. The best performing activator/initiator combinations and concentrations for **4** and **5** resulted in only 12 and 15% decreases in the onset temperature of EVE polymerization, respectively, relative to the thermally initiated polymerization. By comparison, ~75 and 55% decreases were observed for **1** and **2,** respectively. These observations suggest that **4** and **5** may not be reactive enough for the intended application. As such, only the two best performing initiators (**1** and **2**) were used in subsequent experiments.

To simulate the reactivity of various combinations of initiators and activators at body temperature, isothermal DSC experiments were performed at 38 °C. Two additional temperatures (25 °C and 50 °C) were selected to facilitate a more comprehensive evaluation of the temperature dependence of the initial rate of polymerization and the degree of

TABLE 2 Onset Temperature of Polymerization of EVE (°C) by Initiators **1–5** at Two Distinct Concentrations (4.13×10^{-4} mol/g and 8.25×10^{-4} mol/g); and Activators **6–8** (8.25×10^{-5} mol/g and 4.13×10^{-4} mol/g), respectively, as Evaluated by Dynamic DSC (25–300 °C at 10 °C/min)

Initiators (4.13×10^{-4} mol/g)	Activators (8.25×10^{-5} mol/g)		
	6	7	8
1	61	37	36
2	92	71	65
3	116	112	110
4	175	172	159
5	136	135	127

Initiators (8.25×10^{-4} mol/g)	Activators (4.13×10^{-4} mol/g)		
	6	7	8
1	42	<25	<25
2	70	49	42
3	116	101	61
4	170	163	151
5	131	124	115

FIGURE 4 Monomer conversion versus time at various temperatures by various initiators. Polymerization of EVE using combinations of **1** and **6** (a) and **2** and **6** (b). Initiator and activator concentrations are expressed in mol/g resin. The concentration of **6** used was 8.25×10^{-5} mol/g and 4.13×10^{-4} mol/g corresponding to initiator concentrations of 4.13×10^{-4} mol/g and 8.25×10^{-4} mol/g, respectively. [Color figure can be viewed in the online issue, which is available at www.interscience.wiley.com.]
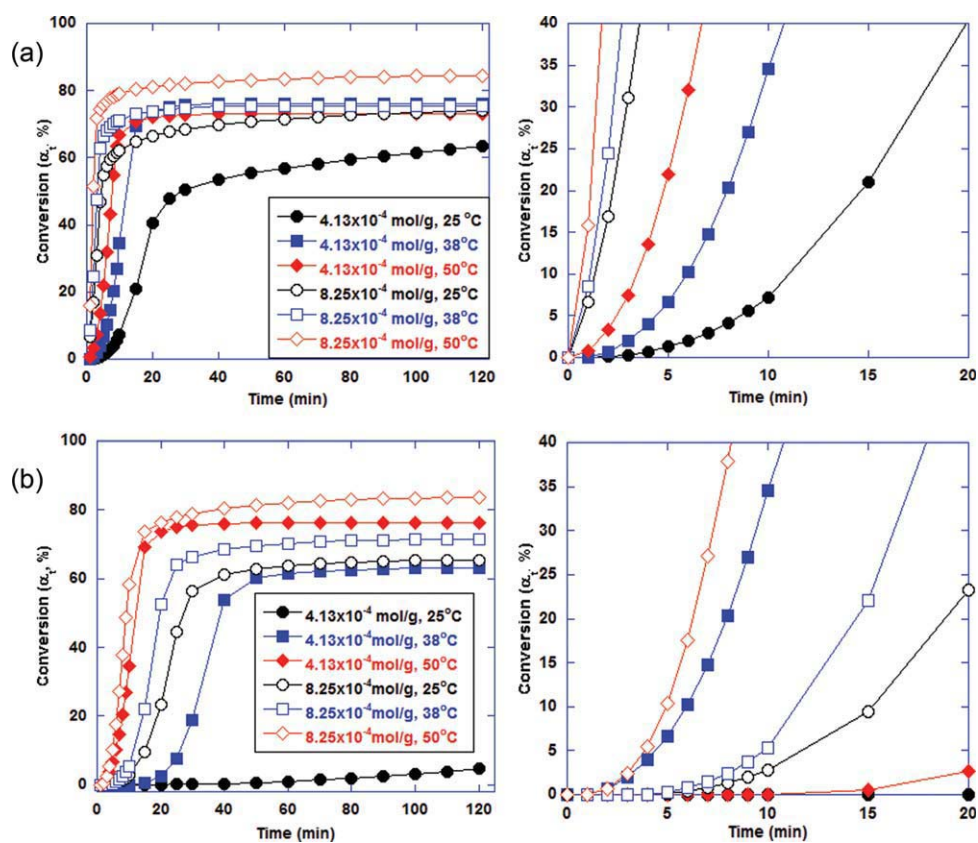
FIGURE 5 Monomer conversion versus time as a function of initiator:activator ratio. Polymerization of epoxy vinyl ester resin using combinations of **1** and **6** (a) and **2** and **6** (b). The initiator and activator concentrations vary between 4.13×10^{-5} mol/g resin and 2.06×10^{-4} mol/g resin for the initiator and 4.13×10^{-6} mol/g resin and 1.65×10^{-3} mol/g resin for the activator. [Color figure can be viewed in the online issue, which is available at www.interscience.wiley.com.]
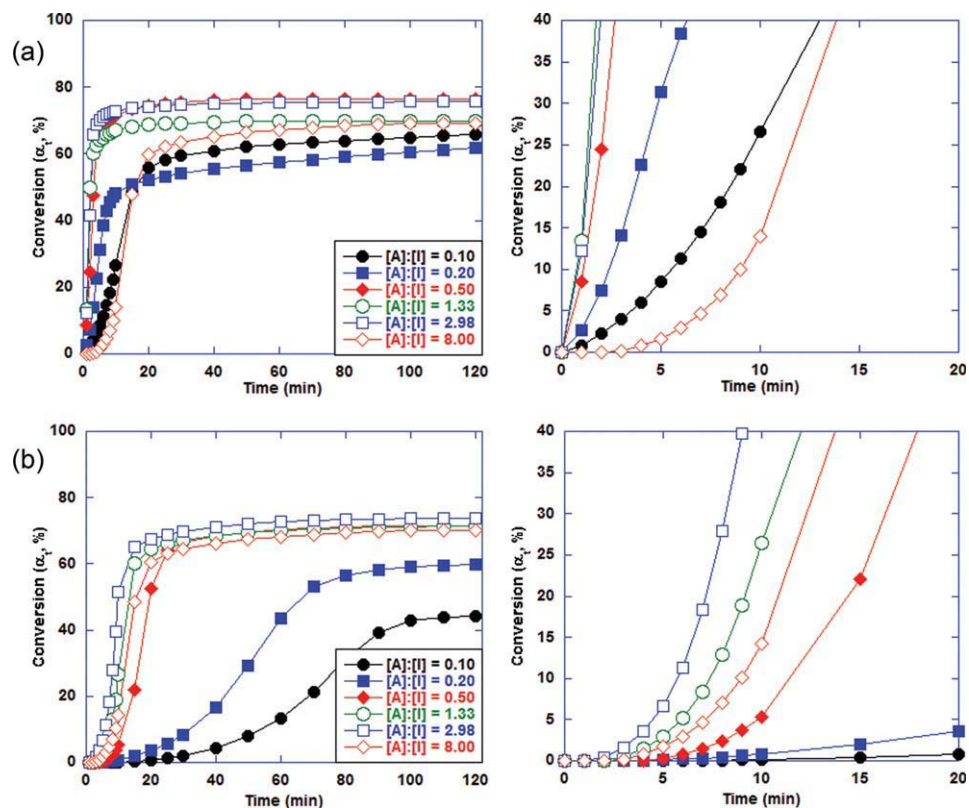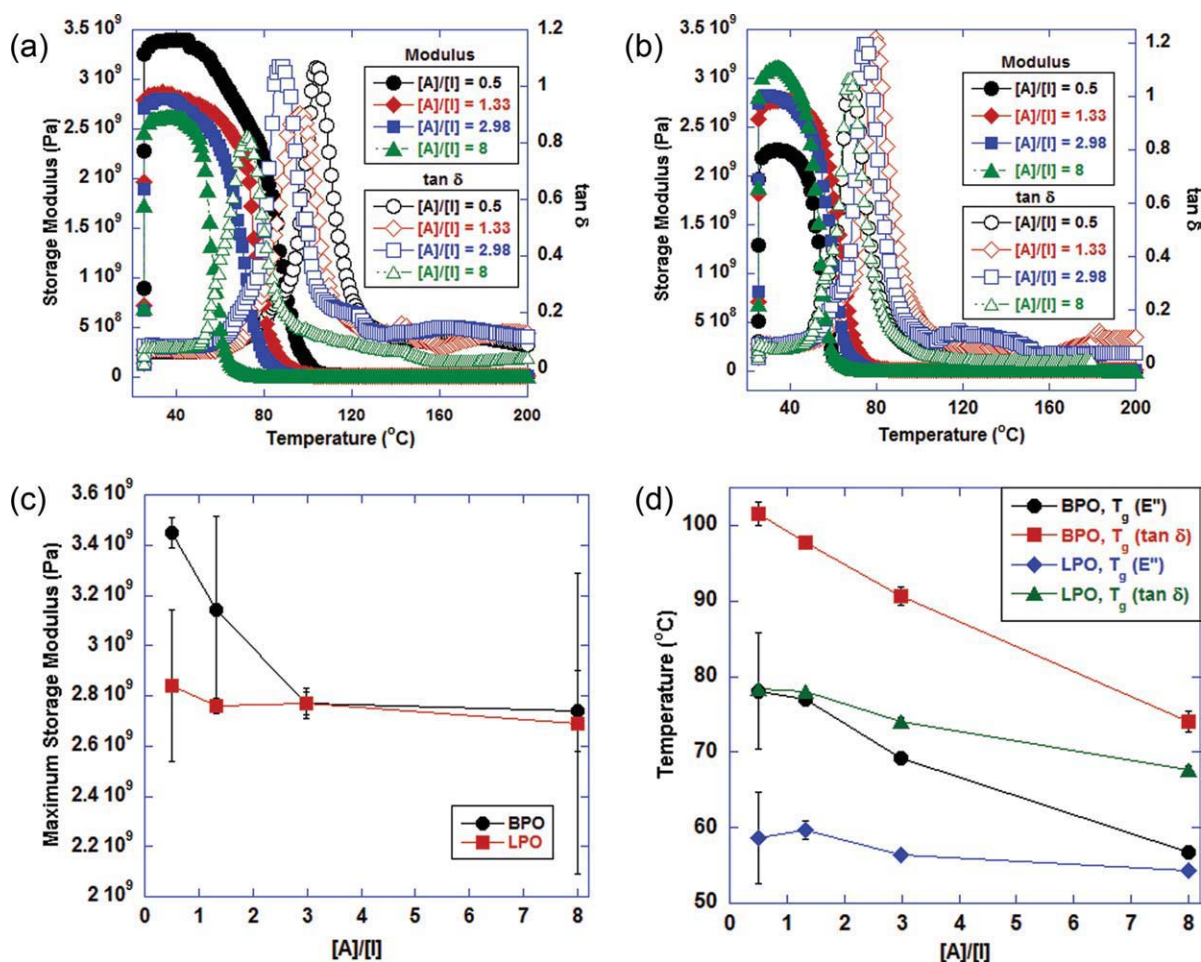
FIGURE 6 Stoichiometric dependence of mechanical properties for EVE cured with various combinations of **1** (BPO) and **6**; and **2** (LPO) and **6**. The initiator and activator concentrations vary between 8.25×10^{-4} mol/g resin and 2.06×10^{-4} mol/g resin for the initiator and 4.13×10^{-4} mol/g resin and 1.65×10^{-3} mol/g resin for the activator. (a) Representative storage modulus (E') and tan δ curves for samples cured with **1** and **6**. (b) Representative storage modulus (E') and tan δ curves for samples cured with **2** and **6**. (c) Comparison of the effect of the ratio of activator/initiator concentrations on the maximum recorded storage modulus. (d) Comparison of the effect of the ratio of activator/initiator concentrations on the T_g determined using the loss modulus and tan δ. The error bars represent one standard deviation based on two trials. [Color figure can be viewed in the online issue, which is available at www.interscience.wiley.com.]

monomer conversion. Initial rate of polymerization and degree of conversion with **1** and **2**, in the presence of DMA as an activator, both generally improved with increasing temperature and concentration of the initiator and DMA (Fig. 4). However, **2** exhibited a much wider range of both initial rate of polymerization and degree of conversion. At 25 °C and a concentration of 4.13×10^{-4} mol/g resin and a DMA concentration of 8.25×10^{-5} mol/g resin, **2** exhibited a small conversion of monomer at the lower concentrations of initiator and activator [Fig. 4(b)], whereas **1** exhibited almost 60% conversion after 2 h under the same conditions [Fig. 4(a)]. At 38 °C, degree of conversion was greater than 60% for both initiators at the two different initiator–activator concentrations. However, initial polymerization rates were significantly different with greater than 60% conversion observed with **1** at both initiator–activator concentrations within the first 10 min, and less than 10% observed with **2** under the

same conditions. Degree of conversion is greater than 75% with both initiators at 50 °C, but **1** still outperforms **2** in initial rate of polymerization.

Effect of Activator/Initiator Ratio

Healing agents released into the crack plane mix at less than optimal concentrations and the effect of stoichiometry on polymerization is important for comparing initiators. The polymerization of the EVE resin at 38 °C was evaluated using a range of activator/initiator concentration ratios ([A]/[I])[22] with DMA as the activator. For this series of experiments, the initiator and activator concentrations were varied between 4.13×10^{-5} mol/g and 2.06×10^{-4} mol/g for the initiator and between 4.13×10^{-6} mol/g and 1.65×10^{-3} mol/g for the activator.

The [A]/[I] ratio had only a small effect on overall monomer conversion with **1** as for all ratios tested, the overall
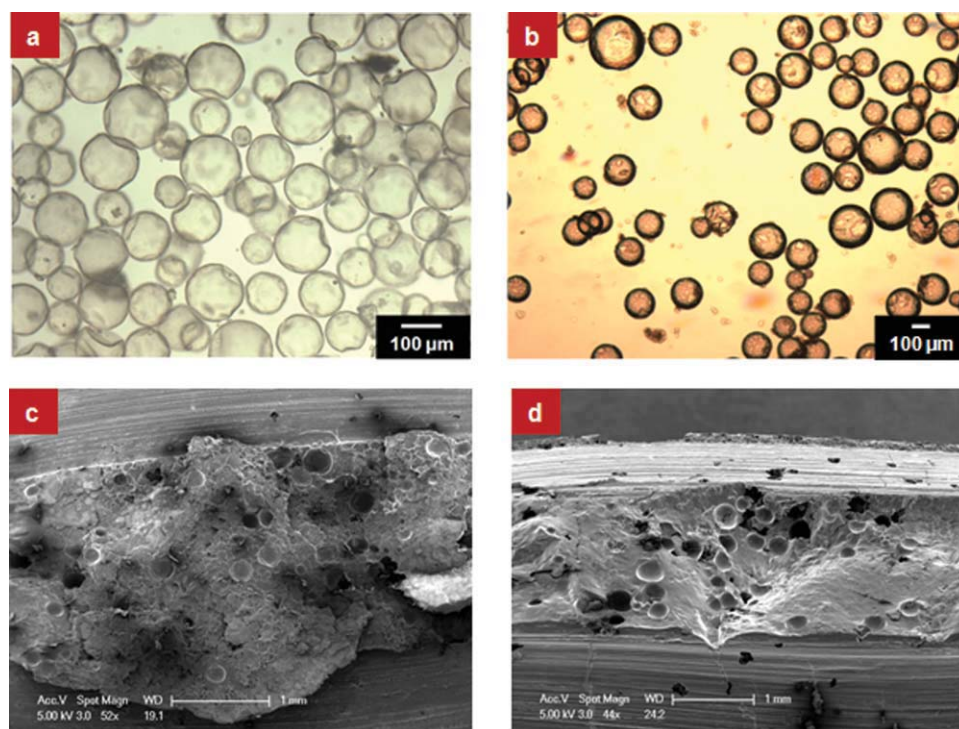
conversion was greater than 60% after 2 h [Fig. 5(a)]. In contrast, the initial polymerization kinetics were more affected by the [A]/[I] ratio. Polymerizations in which the [A]/[I] ratio was between 0.5 and 2.98 all exhibited conversions close to 70% or greater within the first 10 min, while those with [A]/[I] ratios less than 0.5 and greater than 2.98 exhibited conversions of less than 40% in the same time period. Polymerizations with **2** and [A]/[I] ratios less than 0.5 exhibited lower monomer conversions after 2 h as well as marginal conversion within the first 10 min [Fig. 5(b)]. However, in comparison with **1**, **2** did not display as sharp a change in the initial rate of polymerization or the 2 h degree of conversion at an [A]/[I] ratio of 8.00.

The effect of the [A]/[I] ratio on the mechanical properties of the EVE resin polymerized with **1** and **2** using dimethylaniline as the activator was also evaluated. Storage modulus, loss modulus, and tan δ were measured in three-point-bend dynamic mechanical analysis experiments. Representative curves for the storage modulus and tan δ measurements are shown in Figure 6(a,b). On average, samples prepared using **2** exhibited slightly lower moduli than those prepared with **1** [Fig. 6(c)]. The average maximum storage modulus recorded for samples cured with **1** or **2** was greatest at an [A]/[I] ratio of 0.5. However while this [A]/[I] ratio appeared optimal for **1**, **2** was not observed to be as dependent on the [A]/[I] ratio [Fig. 6(c)]. The glass transition temperatures for samples cured with either **1** or **2** determined using the loss modulus and tan δ data were also much more dependent on the [A]/[I] ratio in the case of initiator **1** than with **2** [Fig. 6(d)].

Preliminary Healing Performance

Both initiators were successfully encapsulated using previously reported procedures.[40,41] The resulting capsules are shown in Figure 7(a,b). To facilitate encapsulation and delivery of free-radical initiators, we dissolved a maximum of 9.9 wt % of **1** and 4.3 wt % of **2** into phenyl acetate and hexyl acetate, respectively. These capsules, prepared by saturating the solvent with the initiator, were stored at the desired use temperature (RT) to avoid crystallization at lower temperatures. Encapsulation of higher concentrations of the initiators is possible if the initiators are dissolved into the appropriate solvent at an elevated temperature. However, when the capsules are allowed to cool to temperatures lower than RT for storage, the initiators crystallized from solution destroying the capsule shell wall.

Fracture samples of simulated bone cement were prepared containing both varieties of capsules at 10 vol %. These samples were then fractured on a load frame to ascertain the ability of the capsules to rupture due to crack propagation. The fracture planes for samples prepared with capsules containing **1** [Fig. 7(c)] and **2** [Fig. 7(d)] show that both types of capsules were ruptured during the fracture. The preliminary evaluation of healing performance was then performed in the epoxy vinyl ester resin since it was much more easily molded into repeatable TDCB samples and as discussed earlier, it is functionally analogous to the methacrylate groups found in MMA and Bis-GMA. Because of their superior performance in the kinetics and mechanical analysis experiments, only BPO capsules were evaluated in preliminary healing experiments. Consistent with previously reported data,[46] the addition of BPO capsules resulted in toughening of the matrix up to the maximum concentration of 10 wt %.
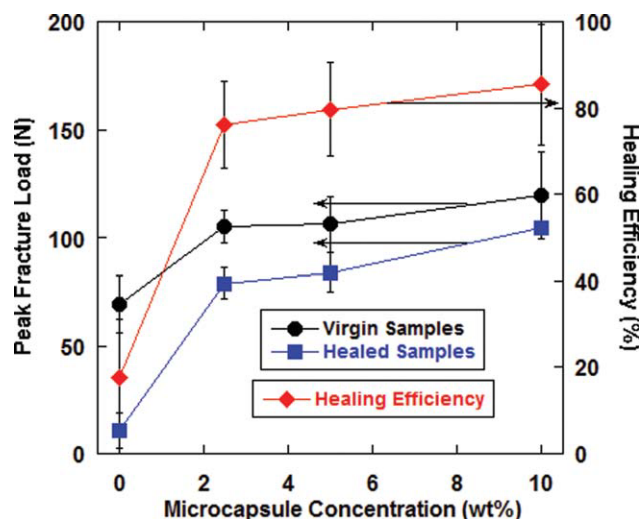
FIGURE 8 Healing performance in EVE samples containing varying concentrations of BPO/PA capsules. A mixture of MMA, EVE, and DMA was injected into the crack plane after the initial fracture. [Color figure can be viewed in the online issue, which is available at www.interscience.wiley.com.]

Samples containing no capsules exhibited a peak fracture load of ~70 N, whereas those containing 10 wt % capsules exhibited peak loads of ~115 N (Fig. 8). After fracture, a mixture

of EVE resin, MMA, and DMA was injected into the fracture plane. Minimal healing was observed in the control sample (efficiencies of ~20%) which did not contain any BPO microcapsules. This observation is likely due to further reaction of the EVE/MMA/DMA mixture with unreacted peroxides promoted by the solvating effects of the MMA. Healing performance was only slightly dependent on the concentration of BPO capsules between 2.5 wt % and 10 wt %. However, the improvement in healing performance (~60%) observed at 2.5 wt % relative to the control is significant. Figure 9 shows the fracture planes resulting from the preliminary healing experiments. The ability of the capsules to rupture in the EVE matrix was first evaluated [Fig. 9(a)]. Figure 9(b) shows the appearance of a polymerized blend of acrylates that was injected into the fracture plane of a neat EVE sample. The difference in appearance of the newly polymerized material on the surface of the EVE fracture plane relative to the EVE matrix alone can be seen by comparing the areas of the EVE matrix not containing microcapsules in Figure 9(a) to the surface of 9(b), which is covered with newly formed polymeric material. Figure 9(c,d) shows an increasing amount of the fracture plane covered by polymerized injected acrylates as the BPO capsule concentration is increased from 5 wt % [Fig. 9(c)] to 10 wt % [Fig. 9(d)]. Ongoing work is focused on the encapsulation of a mixture of acrylic monomers and activators for a fully self-healing system.
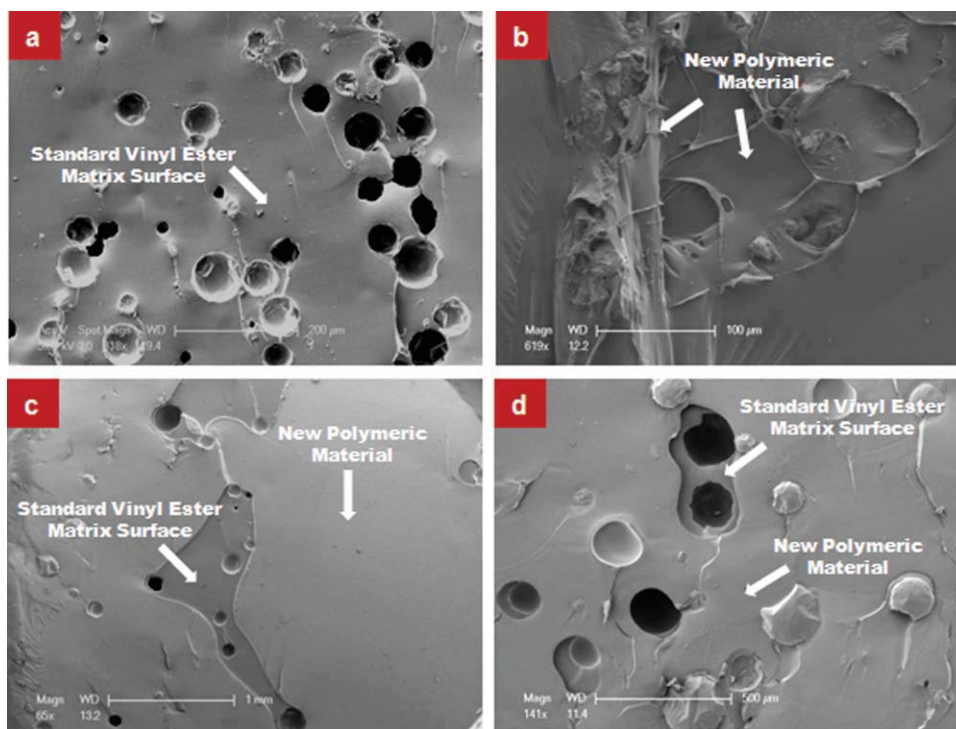
FIGURE 9 EVE fracture planes showing ruptured BPO capsules. (a) Standard EVE fracture plane containing 10 wt % BPO capsules. (b) Healed EVE reference fracture plane containing no capsules, but a mixture of EVE, MMA, DMA (0.1 wt %), and BPO (1 wt %) was injected into the fracture plane after the virgin fracture. New polymeric material can be seen on the surface. (c) EVE fracture plane containing 5 wt % BPO capsules. A mixture of EVE, MMA, and DMA was injected into the fracture plane after the virgin fracture. (d) EVE fracture plane containing 10 wt % BPO capsules. A mixture of EVE, MMA, and DMA was injected into the fracture plane after the virgin fracture. [Color figure can be viewed in the online issue, which is available at www.interscience.wiley.com.]

CONCLUSIONS

Five common peroxide initiators with a range of physical properties were selected for evaluation for potential application in a free-radical polymerization-based self-healing system. The initiators were evaluated for thermal stability, reactivity, stoichiometric dependence, and compartmentalization. Initiator **1** emerged as the best performing initiator over the range of the evaluation criteria. The initiator was successfully dissolved in phenyl acetate and microencapsulated in urea-formaldehyde microcapsules. The capsules were then incorporated into EVE resin samples for evaluation of the healing potential of the encapsulated initiator. The samples containing the initiator capsules exhibited upwards of 80% healing efficiency when they were fractured and a mixture of MMA, EVE, and DMA was injected into the crack plane. The encapsulation of initiators **1** and **2** could also find application in frontal polymerizations.[47,48]

REFERENCES AND NOTES

1 White, S. R.; Sottos, N. R.; Geubelle, P. H.; Moore, J. S.; Kessler, M. R.; Sriram, S. R.; Brown, E. N.; Viswanathan, S. Nature 2001, 409, 794–797.

2 Cho, S. H.; Andersson, H. M.; White, S. R.; Sottos, N. R.; Braun, P. V. Adv Mater 2006, 18, 997–1000.

3 Cho, S. H.; White, S. R.; Braun, P. V. Adv Mater 2009, 21, 645–649.

4 Keller, M. W.; White, S. R.; Sottos, N. R. Adv Funct Mater 2007, 17, 2399–2404.

5 Caruso, M. M.; Delafuente, D. A.; Ho, V.; Sottos, N. R.; Moore, J. S.; White, S. R. Macromolecules 2007, 40, 8830–8832.

6 Caruso, M. M.; Blaiszik, B. J.; White, S. R.; Sottos, N. R.; Moore, J. S. Adv Funct Mater 2008, 18, 1898–1904.

7 Therriault, D.; White, S. R.; Lewis, J. A. Nat Mater 2003, 2, 265–271.

8 Toohey, K. S.; Sottos, N. R.; Lewis, J. A.; Moore, J. S.; White, S. R. Nat Mater 2007, 6, 581–585.

9 Toohey, K. S.; Sottos, N. R.; White, S. R. Exp Mech 2009, 49, 707–717.

10 Toohey, K. S.; Hansen, C.; Sottos, N. R.; Lewis, J. A.; White, S. R. Adv Funct Mater 2009, 19, 1399–1405.

11 Hansen, C. J.; Wu, W.; Toohey, K. S.; Sottos, N. R.; White, S. R.; Lewis, J. A. Adv Mater 2009, 21, 4143–4147.

12 Pang, J. W. C.; Bond, I. P. Compos Sci Technol 2005, 65, 1791–1799.

13 Pang, J. W. C.; Bond, I. P. Compos A 2005, 36, 183–188.

14 Chen, X.; Wudl, F.; Mal, A. K.; Shen, H.; Nutt, S. R. Macromolecules 2003, 36, 1802–1807.

15 Chen, X.; Dam, M. A.; Ono, K.; Mal, A.; Shen, H.; Nutt, S. R.; Sheran, K.; Wudl, F. Science 2002, 295, 1698–1702.

16 Peterson, A. M.; Jensen, R. E.; Palmese, G. R. ACS Appl Mater Interfaces 2009, 1, 992–995.

17 Kessler, M. R.; Sottos, N. R.; White, S. R. Compos A 2003, 34, 743–753.

18 American Academy of Orthopedic Surgeons Patient Demographics Page. Available at: www.aaos.org/research/stats/patientstats.asp (Accessed: October 2009).

19 Lewis, G. J Biomed Mater Res 1997, 38, 155–182.

20 Lewis, G. J Biomed Mater Res 2008, 84B, 301–319.

21 Wilson, G. O.; Moore, J. S.; White, S. R.; Sottos, N. R.; Andersson, H. M. Adv Funct Mater 2008, 18, 44–52.

22 Bowen, R. L.; Argentar, H. J Appl Polym Sci 1973, 17, 2213–2222.

23 Deb, S.; Lewis, G.; Janna, S. W.; Vazquez, B.; San Roman, J. J Biomed Mater Res 2003, 67A, 571–577.

24 Milner, R. J Biomed Mater Res 2004, 68B, 180–185.

25 Charnley, J. J Bone Joint Surg 1960, 42B, 28–30.

26 Vazquez, B.; Elvira, C.; Levenfeld, B.; Pasqual, B.; Goñi, I.; Gurruchaga, M.; Ginebra, M. P.; Gil, F. X.; Planell, J. L.; Liso, P. A.; Rebuelta, M.; San Roman, J. J Biomed Mater Res 1997, 34, 129–136.

27 Liso, P. A.; Vázquez, B.; Rebuelta, M.; Hernáez, L.; Rotger, R.; San Román, J. Biomaterials 1997, 18, 15–20.

28 Elvira, C.; Levenfeld, B.; Vázquez, B.; San Román, J. J Polym Sci Part A: Polym Chem 1996, 34, 2783–2789.

29 de la Torre, B.; Fernández, M.; Vázquez, B.; Collìa, F.; de Pedro, J. A.; López-Bravo, A.; San Román, J. J Biomed Mater Res 2003, 66B, 502–513.

30 Vázquez, B.; San Román, J.; Deb, S.; Bonfield, W. J Biomed Mater Res 1998, 43B, 131–139.

31 Vázquez, B.; Deb, S.; Bonfield, W.; San Román, J. J Biomed Mater Res 2002, 63B, 88–97.

32 Harper, E. J.; Behiri, J. C.; Bonfield, W. J Mater Sci Mater Med 1995, 6, 799–803.

33 Clarke, R. L.; Braden, M. J Dent Res 1982, 61, 1245–1249.

34 Borzacchiello, A.; Ambrosio, L.; Nicolais, L.; Harper, E. J.; Tanner, K. E.; Bonfield, W. J Mater Sci Mater Med 1998, 9, 317–324.

35 Müh, E.; Zimmerman, J.; Kneser, U.; Marquardt, J.; Mülhaupt, R.; Stark, B. Biomaterials 2002, 23, 2849–2854.

36 Dalby, M. J.; Di Silvio, L.; Harper, E. J.; Bonfield, W. Biomaterials 2002, 23, 569–576.

37 Shinzato, S.; Kobayashi, M.; Mousa, W. M.; Kamimura, M.; Neo, M.; Kitamura, Y.; Kokubo, T.; Nakamura, T. J Biomed Mater Res 2000, 51, 258–272.

38 Shinzato, S.; Nakamura, T.; Kokubo, T.; Kitamura, Y. J Biomed Mater Res 2001, 54, 491–500.

39 Wilson, G. O.; Caruso, M. M.; Reimer, N. T.; White, S. R.; Sottos, N. R.; Moore, J. S. Chem Mater 2008, 20, 3288–3297.

40 Brown, E. N.; Kessler, M. R.; Sottos, N. R.; White, S. R. J Microencapsulation 2003, 20, 719–730.

41 Blaiszik, B. J.; Caruso, M. M.; McIlroy, D. A.; Moore, J. S.; White, S. R.; Sottos, N. R. Polymer 2009, 50, 990–997.

42 Brown, E. N.; Sottos, N. R.; White, S. R. Exp Mech 2002, 42, 372–379.

43 Table entries summarized from the MSDS information provided by the manufacturers of the respective the initiators.

44 Hatakeyama, T.; Quinn, F. Applications of Thermal Analysis: Fundamentals and Applications to Polymer Science, 2nd ed.; Wiley: Chichester, England, 1994.

45 Kostoryz, E. L.; Tong, P. Y.; Chappelow, C. C.; Eick, J. D.; Glaros, A. G.; Yourtee, D. M. Dent Mater 1999, 15, 363–373.

46 Brown, E. N.; White, S. R.; Sottos, N. R. J Mater Sci 2004, 39, 1703–1710.

47 McFarland, B.; Popwell, S.; Pojman, J. A. Macromolecules 2004, 37, 6670–6672.

48 McFarland, B.; Popwell, S.; Pojman, J. A. Macromolecules 2006, 39, 53–63.